MASTER THESIS

EFFECTS OF SHORT-TERM BODY-WEIGHT SUPPORT TRAINING ON SOLEUS MOTOR UNIT BEHAVIOUR

Alexandra Millar

UNIVERSITY OF TWENTE.

31-08-2023

Effects of short-term body-weight support training on soleus motor unit behaviour

Alexandra Millar

Abstract—Gait impairment arises from a range of conditions, many of which fall under the umbrella of central nervous system injury. Central nervous system disorders are one of the largest contributors to disability worldwide and stem from a multitude of causes ranging from genetic disorders to traumatic injuries. A variety of treatment options exist for individuals with central nervous system disorders. These treatments can range from manual physiotherapy to gait training using robotic interventions such as body-weight support. Body-weight support is a rehabilitative tool that can support patients over a wide variety of tasks from simple treadmill walking to dynamic actions such as climbing stairs. While extensive research has been done to evaluate the physiological outcomes of body-weight support training, there is limited understanding of the underlying neurophysiological adaptations that drive these changes. The soleus stretch reflex is one window into the motor unit behaviour that drives gait and balance. By examining the effects of short-term body-weight support training on motor unit behaviour, further insights into the kinematic improvements of patients may be understood. In this study, the soleus short latency reflex response is selected as a method of evoking motor unit discharges. The reflex is evoked by administering approximately 80 dorsiflexion perturbations while the subject maintains 20% of their maximum voluntary contraction. This perturbation protocol is administered once as a baseline measurement and compared to recordings taken after training with the ZeroG body-weight support system at 40% gravity compensation and unassisted treadmill walking. Electromyography data is recorded using a high-density sensor grid during the perturbation protocols, and decomposed into motor unit innervation pulse trains using Convolution Kernel Compensation. Peri-stimulus time histograms and frequency-grams are used to extract the latency, amplitude, duration, and mean discharge rate of the short latency reflex from the decomposed motor unit data. A total of 99 motor units were pooled across subjects and recordings. No changes were found in the pooled data, however, an analysis of individual motor units tracked between recordings indicated that there may be an increase in latency after training with body-weight support. This limited but promising result suggests that the analysis of individual motor units may hold the keys to unlocking overarching motor unit behaviour.

I. INTRODUCTION

Gait impairment as a result of a central nervous system (CNS) disorder is increasingly prevalent in the global society, with neurological disorders being the leading cause of disabilities worldwide [1][2]. CNS disorders that affect gait include, but are not limited to, cerebrovascular injury (CVA), spinal cord injury (SCI), traumatic brain injury, Parkinson's disease and multiple sclerosis. These disorders can affect the individual's balance and muscle spasticity, leading to difficulty walking and interacting with their surroundings [3]. This in turn puts an emotional and financial burden on the patient, as they may require life-long assistance to navigate everyday scenarios. Currently, a variety of rehabilitation methods for CNS disorders exist, ranging from manual physiotherapy to robotic-assisted therapy, with many focusing on the improvement of balance and gait [4].

Methods of rehabilitation are ever-improving and evolving, however, historically there has been an emphasis on the clinical outcome of rehabilitation with little insight into the underlying physiological adaptations [5]. At this time, there is little agreement between researchers as to the most effective approach to CNS rehabilitation [6]. The traditional approach to gait rehabilitation has been to address the physical symptoms with the aim of influencing the neural system [3]. Typically, gait rehabilitation sessions consist of repetitive actions completed with the assistance of either a physiotherapist or an assistive device [7]. At this time, lower-limb rehabilitation assistive devices may range from crutches or canes to treadmill walking to body-weight support. Training sessions may be repeated over a period of days, months, or even years. Training protocols are simultaneously varied in their content, while applied in the same manner to patients regardless of the patient's impairment [5][6]. There is a lack of research into how training protocols should account for conflicting considerations of either improvement after injury (for instance post-stroke or SCI) or mitigation of disease progression, in the case of Parkinson's and multiple sclerosis [5]. There is growing evidence to suggest that individualized, targeted, training produces the best rehabilitative results [8][9].

In terms of assistive devices for improving balance and gait, exoskeletons and body-weight support (BWS) devices are the current state of the art, with a report finding that of 316 studies analyzed, the majority of robotic interventions targeting the lower limbs were exoskeletons [5]. Both exoskeletons and BWS devices work by lowering the amount of force the patient needs to generate in order to complete a task. Reducing the load on the patient's limbs can decrease the muscle forces throughout the lower limbs, as well as the aerobic requirements of patients to complete such tasks [10][11]. Exoskeletons achieve this by adding mechanical power to a particular joint or joints, such as the knee or ankle. In the case of SCI patients, training using an exoskeleton has been shown to improve walking kinematics and locomotor ability, and neurophysiological changes at the spinal and supraspinal level have been shown [12][13]. In healthy subjects, short-term training using an exoskeleton has shown a reduction in muscle activation [14][15]. Body-weight support works by reducing the effects of gravity on the patient's limbs [10]. Through training, the patient can regain strength or re-learn how to execute certain actions [6][16]. Long-term use of BWS training by chronic SCI patients has shown promising results, with significant increases in functional walking abilities [17]. BWS appeals to both clinicians and researchers as it is typically simple to use and can be easily adjusted to a wide range of subjects and training scenarios. While the physiological outcomes have been thoroughly studied, the underlying mechanisms

guiding these outcomes are still not well understood [5]. By gaining a better understanding of how such training affects the neurophysiological system, targeted training plans could be developed to improve their outcome.

Many individuals with a CNS disorder exhibit abnormally high stretch reflexes that prohibit them from walking with a typical gait [14]. There are two reflexes commonly studied in the soleus muscle, the stretch reflex and the Hoffman (H-) reflex. The stretch reflex is comprised of several successive bursts of excitation, known as the short-, medium-, and long-latency responses [18]. These bursts are also respectively referred to as the M1, M2, and M3 responses [19]. The M1 response is the first to appear and is primarily generated by group Ia afferents [19]. The M2 response has contributions from group Ib and II afferents, and the M3 response may be mediated by transcortical pathways [18][19][20]. The H-reflex is the electrical analogue to the M1 response, and is induced by electrically stimulating the relevant nerve. The H-reflex can be used to quantify the excitability of alpha-motoneurons as it elicits a direct response from the spinal pathway and is composed almost entirely of Ia afferents [19][21][22]. The stretch reflex, however, also includes contributions from the muscle spindle otherwise bypassed by the H-reflex.[19]. One benefit of studying the stretch reflex is that it more accurately reflects natural behaviour. Since a main application of this research is to gait training, contributions from the muscle spindle sensitivity should also be considered. From a purely practical level, the stretch reflex is simple to evoke and requires very little inter-patient tuning when compared to the electrically induced H-reflex. During this thesis, the M1 response of the soleus muscle will be examined for its insight into afferent activity[19]. The soleus muscle is essential for both stance and motion due to its role as a plantarflexor of the ankle joint. The ability to understand and tune the effects of training this muscle could therefore have a significant impact on patients' balance. The soleus stretch reflex is elicited by applying a rapid dorsiflexion perturbation to the ankle joint with the M1 response being the first peak to appear after the ankle joint is perturbed.

Four parameters can be used to describe the motor unit response; the latency, amplitude, and duration of the M1 response, and the motor unit discharge rate. Latency is the time between the perturbation and the onset of the M1 reflex, and can be considered a measure of the synaptic delay. Amplitude is the difference in height of the reflex between the onset and the peak of the M1 response when observed in the frequency domain. The amplitude gives an indication of the strength of the afferent input. The duration is the time between the onset of the reflex and the first plateau of the response and reflects the response time of the reflex system. It has been found that latency is influenced by the muscle spindle sensitivity, and can be modulated during isometric contractions by the ankle angle [23]. Latency does not change with respect to ankle angle during normal walking, which is postulated to be due to the muscle spindle modulation [23]. Both amplitude and duration have been shown to

be influenced by the contraction force during isometric contractions [24]. The motor unit discharge rate has also been found to increase with contraction intensity during isometric contractions [25].

While previous studies have examined the reflex behaviour of the soleus muscle after short-term training with body-weight support, these studies have used bipolar surface electromyography (sEMG) to examine the H-reflex, without looking directly into the underlying motoneuron activity [14][26]. Intramuscular electromyography has typically been used to directly measure motor unit action potentials, however, this is an invasive method that is limited to a small area of the muscle and can only detect a small number of motor units [27][28]. Spike-triggered averaging is a method often used in EMG-based reflex studies[29][30]. This method requires averaging EMG data across the timing of spike occurrences and consequently is susceptible to amplitude cancellation and motor unit synchronization[31]. Studying individual motor units circumvents these limitations of global EMG data. High-density surface electromyography (HD-EMG) provides a non-invasive method of examining the underlying changes at the muscular level. Gradient Convolution Kernel Compensation (CKC) offers the opportunity to directly measure motoneuron activity when used in conjunction with HD-EMG. The use of gradient CKC allows for the decoding of individual motor unit innervation pulse trains from HD-EMG data and has been shown to be robust to noise [32].

Thus, the aim of this thesis was to determine whether the use of high-density electromyography in conjunction with cross-kernel convolution could provide sufficient statistical power to gain insight into the underlying neurophysiological adaptations to body-weight support training. By understanding how to manipulate the stretch reflex using body-weight support, specific training stratagems can be developed to help bring atypical reflexes in injured patients toward the desired level.

II. METHODS

A. Subject Preparation

Six healthy subjects (5 male, 1 female) volunteered to participate in the experiment. Subjects provided their written consent in accordance with the University of Twente Ethics Committee. The subject's right medial soleus muscle was first located by muscle palpation, and then the area was shaved and cleaned using isopropyl alcohol. The area was then gently abraded using an abrasive gel. A high-density surface electromyography grid (TMSi; Oldenzaal, Netherlands) was then placed on the belly of the soleus using a double-sided adhesive. The sensor consists of an eight-by-eight array of monopolar EMG sensors with a 4mm inter-electrode distance. The HD-EMG grid was then further secured using tape over the grid to ensure even contact between the sensors and the skin across the muscle and to prevent the grid from slipping during the protocol.
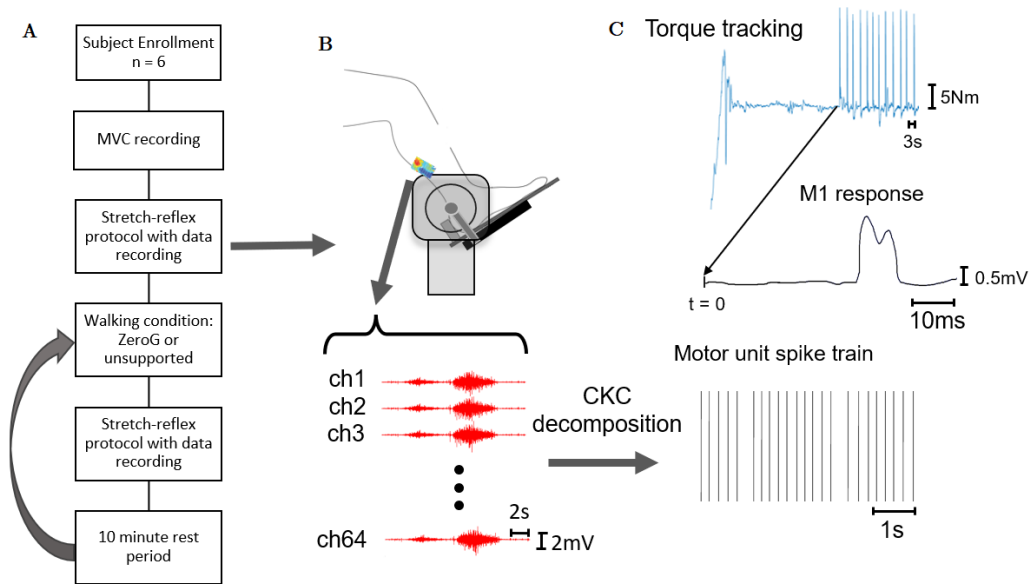
Fig. 1: Schematic of the experimental protocol. A: Overview of the experimental protocol. B: HD-EMG data is recorded from the medial soleus muscle during the stretch-reflex protocol. C: Perturbations duration the torque-tracking component of the stretch-reflex protocol are used to elicit the M1 motor unit response, which can be observed in the HD-EMG data. The HD-EMG data is then decomposed into motor unit spike trains using a cross-kernel convolution algorithm.

B. Data Collection

The experiment was set up as a crossover study in which the order the subjects underwent the intervention or control training was randomized. Of the six subjects enrolled, four first completed the ZeroG (intervention) training, and two first completed the unassisted walking control. Data was collected during a stretch-reflex protocol upon subject arrival, and after both the ZeroG and unassisted walking tasks. Figure 1 gives an overview of the experimental protocol.

1) EMG Recording: Electromyography data was collected during a stretch-reflex protocol at 2048 Hz using a REFA (TMSi; Oldenzaal, Netherlands) EMG amplifier. The subject's maximum voluntary contraction (MVC) was measured upon subject arrival using a Biodex dynamometer (Biodex Medical Systems, Inc.; Shirley, New York, USA). The MVC was taken to be the maximal peak from three consecutive contractions. Torque, position, and velocity data were also recorded at this time using the Achilles ankle perturbator (MOOG; Nieuw Vennep, Netherlands). Subjects were seated in the Achilles with the backrest and foot-rest angles adjusted such that the subjects' maintained a knee angle of 120 degrees and ankle angle of 90 degrees. During the stretch-reflex protocol, the subject was prompted to follow a torque-based ramp and hold tracking task, with a ramp peaking at 30% MVC, and the hold being maintained at 20% MVC. This level of sustained contraction was chosen to limit the potential of muscle fatigue during recording and to maximize the number of motor units that could be decomposed [25]. During the hold section of the task, approximately 75 dorsiflexion perturbations were applied using the Achilles at a randomized interval of two to three seconds over 200 seconds. As the data analysis

requires the averaging of data with respect to the number of perturbations, this amount of stimuli should ensure that the results are accurate [33]. The perturbation was a 0.08 rad change in position with a peak velocity of 3.3 rad/s and a pulse duration of 0.24s. The stretch-reflex protocol was administered upon subject arrival, this initial recording will henceforth be called the baseline recording, and after both the ZeroG training session and walking control session. Subjects were permitted two attempts at the task for the baseline measurement to allow the subject to become familiar with following the tracking task.

2) Walking tasks: During the ZeroG and unassisted walking control tasks subjects were asked to walk at a continuous self-selected walking speed. Subjects were directed to walk as if they were taking a long walk through a park- the pace should be comfortable and possible to maintain for all 30 minutes of the trial. Subjects walked at speeds ranging from 2.4-3.0 kilometers per hour. The cadence was controlled between the ZeroG and control tasks using Metronome Beats (Stonekick; London, UK) an app-based metronome. Speed was controlled using the treadmill settings. The ZeroG Gait and Balance system (Aretech, LLC; Ashburn, Virginia, USA) is a device used for both rehabilitation and research [10]. This device works by dynamically supporting a person using a harness attached to a robot that travels on a ceiling-mounted track. The user can select the amount of weight to compensate for, allowing the patient to support themselves to a specified degree and perform tasks such as sitting, standing, walking, and climbing stairs. During the ZeroG tasks subjects walked at 40% weight compensation. Literature suggests that this level of weight compensation provides the largest decrease in muscle activation without compromising the subject's natural walking pattern [11] [26]. Subjects were instructed to walk for

a minimum of two minutes with the ZeroG providing support to become comfortable with the application of the weight compensation. When the subject was ready, the 30 minutes of training began. No subject walked for more than 35 minutes during the ZeroG training. For the control portion subjects walked on the treadmill without any support from the ZeroG apparatus for 30 minutes.

C. Data Analysis

The EMG data was analyzed offline using MATLAB R2020a (The Mathworks Inc.; Natick, USA). The EMG and Achilles perturbator data were first aligned using a synchronization channel and the corresponding Achilles signal, such as the position, to measure the offset between the two devices. During data post-processing, it was found that the majority of EMG data showed a linearly increasing lag. The affected data was resampled accordingly in a process that is further described in Appendix A.

The quality of the raw EMG data was first checked by evaluating the power spectral density for each channel. The EMG data was then filtered using a 50 Hz Notch filter to remove power line noise, and a fourth-order Butterworth zero-lag filter with cut-off frequencies of 20 Hz and 500 Hz was applied. The data was then evaluated for a-typical peaks in frequency by once again examining the power spectral density for each channel, and specific notch filters were applied per data set to remove any further contamination. Channels with poor electrode-skin impedance (no signal recorded) were then removed from the data set, and the decomposition algorithm was applied.

The motor unit spike trains were extracted using DEMUSE (The University of Maribor; Maribor, Slovenia) a MATLAB-based convolutive blind source separation software [32]. The data was segmented into 60-second epochs with a ten-second overlap between windows. Segmenting the data into epochs decreases the processing time and amount of noise in the motor units decomposed. The decomposed spike trains were then merged using a cross-correlation algorithm that mapped spike trains in adjacent epochs to each other using a threshold level of 85% correlation [24]. The first of the four features used in this thesis to analyze motor unit behaviour was extracted at this time. This feature is the mean discharge rate, which can be defined mathematically as the inverse of the interspike interval [34]. One subject's (S3's) data was decomposed as a whole, due to the presence of bursts of noise throughout all three recordings for this subject that interfered with the epoch decomposition method.

1) Pooled Motor Units: Peri-stimulus time histogram (PSTH) and peri-stimulus frequency-gram (PSF) analyses were performed. The PSTH gives the number of motor unit spike occurrences within a set time window around the stimulus [35]. In this instance the time window ranged from 200ms before the perturbation to 250ms after the perturbation. This is a longer pre-stimulus time window than the typical 50ms

prior to stimulus. The 200ms was chosen due to the high noise level in the decomposed motor unit data, as the reflex is represented against an estimated baseline based on data in the pre-stimulus time window. The PSF compares the instantaneous discharge rates of single motor units against the time instant of the stimulus [24]. Both methods are also analyzed with their respective cumulative sums, which can be mathematically described as:

$$CUSUM(t_{pre}) = 0$$

$$CUSUM(t) = \sum_{t_{pre}}^{t_{post}} (x(t) - M) \qquad (1)$$

where $x(t)$ is the instantaneous discharge rate at time t and M is the mean pre-stimulus discharge rate. t_{pre} and t_{post} give the respective beginning and end time the peri-stimulus window. The use of cumulative sums can reveal small changes otherwise undetectable in the PSTH or PSF methods [35].

Using the peri-stimulus cumulative sum frequency-gram (PSFC) three of the four features used to evaluate motor unit behaviour in this thesis were extracted. The features are the latency, amplitude, and duration. The M1 onset is defined as the first change in direction of the PSFC curve after the perturbation is applied. The latency is then measured as the difference between the perturbation time and the reflex onset. The peak of the M1 response is considered the next change in direction, or "plateau" of the PSFC curve. The duration is determined as the time period between the onset and plateau of the M1 response. The amplitude is taken as the distance between the onset and plateau of the curve. Figure 2 illustrates how these features are determined using the PSFcusum. Motor units without a clear M1 response or excessive noise in the pre-stimulus window were eliminated from the analysis at this time.
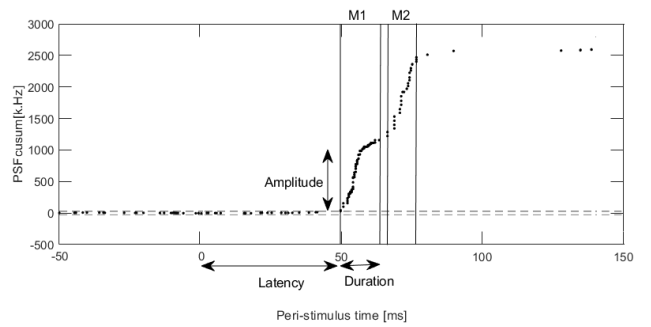

Fig. 2: Example of PSFC curve showing the M1 and M2 reponses. The beginning and end points of the M1 and M2 responses are indicated by the solid vertical lines. The latency, amplitude, and duration have also been indicated using double arrows. The dashed horizontal lines give the baseline used to determine the significance level of the reflex response. A shortened window of -50ms to 150ms is shown in the figure for clarity

In order to control for between-subject effects the results from this peri-stimulus analysis were then z-score normalized and the normalized data was pooled for further analysis. The formula for z-score normalization is as follows:

$$Z = \frac{x - \mu}{\sigma} \tag{2}$$

Where Z is the normalized value, x is the observed value, μ is the mean value of all motor units per subject per trial, and σ is the standard deviation of the value for all motor units per subject per trial.

2) Tracked Motor Units: The decomposed motor unit spike trains were matched between conditions using a two-dimensional cross-correlation as described by Martinez-Valdez et al. [36]. This method uses spike-triggered averaging to compare the action potentials of two motor units for all 64 channels of the HD-EMG sensor. In other words, for each channel an average action potential was generated by averaging every 50 milliseconds of the filtered EMG signal for the duration of the corresponding motor unit spike train for each motor unit. For each condition, every motor unit was compared against each motor unit of the next condition, and the greatest cross-correlation between the two motor unit action potentials (MUAPs) was recorded. For this analysis, a threshold of 85% cross-correlation was used.

Muscle fatigue between trials was checked for by comparing the discharge rate over time of matched MUs for the post-ZeroG and post-control conditions to the baseline condition. A trend of increasing discharge rates over time when compared to the baseline condition would indicate that the muscle was experiencing fatigue [37].

D. Statistical Analysis

Statistical testing was performed using IBM SPSS Statistics v.27 (IBM Corporation, New York, USA). A linear mixed-effects analysis was fitted to the observed data values, as these were measured across three separate conditions which were measured consecutively. The trial condition (baseline, post-ZeroG, or post-control) was considered a fixed effect, and the subjects were defined as a random effect. The level of significance was $P < 0.05$. Descriptive statics include the mean and standard deviation per subject for each feature.

III. RESULTS

A. Pooled Motor units

A total of 31 motor units were pooled for the baseline condition, 33 motor units for the post-ZeroG condition, and 36 for the post-control condition. 31 motor units from the baseline and post-ZeroG conditions and 32 motor units for the post-control condition were included in the z-score normalization. The number of motor units decomposed per subject varied between conditions by a minimum of 1 motor unit, and a maximum of eight motor units.

The averaged latency, amplitude, duration, and mean discharge rates were measured for each motor unit. Figure 3 gives the observed latency in Figure A and the observed amplitude in Figure B. Figure 4 gives the observed duration and mean discharge rate for Figures A and B respectively. Looking further into each feature, it can be seen that the range of the observed latency decreases for subjects one, three, four, and five. Subject six shows an increased range for both the post-ZeroG and post-control conditions. When subject effects are considered there is no significant change in latency between conditions (P = 0.087).
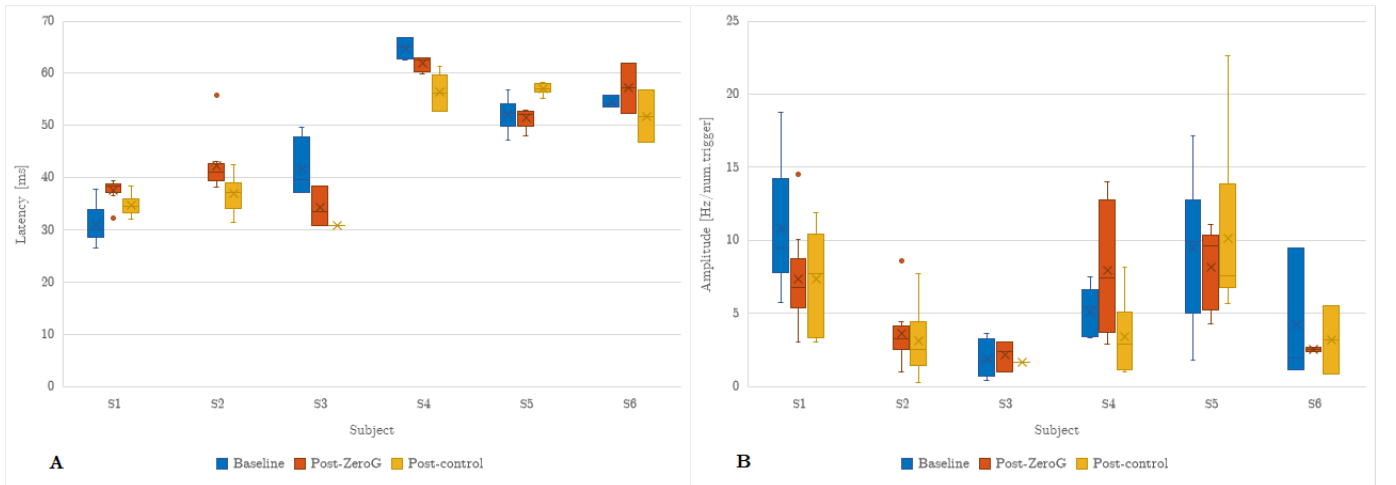

Fig. 3: A: Observed latency for all subjects across all three conditions; B: Observed amplitude for all subjects across all three conditions. The whiskers indicate the maximum and minimum values of the data. The upper limit of the box indicates the median of the third quartile, while the lower limit of the box gives the median of the first quartile. The horizontal line within the box gives the median of the whole, and the X indicates the mean of the whole. Outliers are indicated with dots.
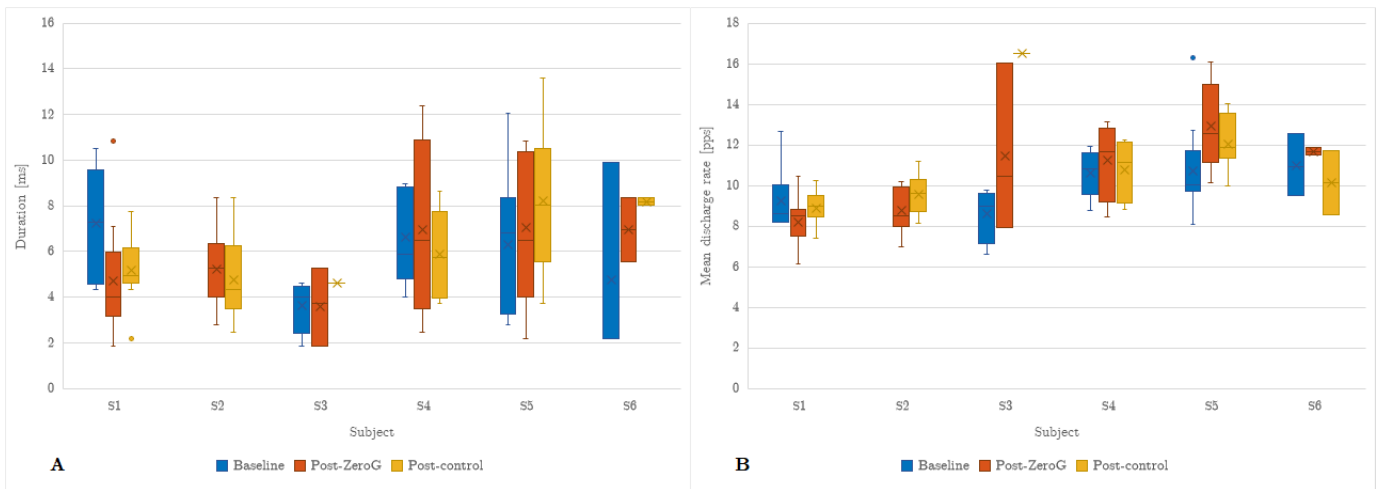
Fig. 4: A: Observed duration for all subjects across all three conditions; B: Observed mean discharge rate for all subjects across all three conditions. The whiskers indicate the maximum and minimum values of the data. The upper limit of the box indicates the median of the third quartile, while the lower limit of the box gives the median of the first quartile. The horizontal line within the box gives the median of the whole, and the X indicates the mean of the whole. Outliers are indicated with dots.

The range of the observed amplitude decreases between the baseline and Zero-G conditions for subjects one, three, five, and six. These changes are not considered significant, with $P = 0.418$. It can be seen that there is no distinguishable trend in the duration between the baseline and post-ZeroG or post-control values (duration: $P = 0.878$; discharge rate: $P = 0.129$). The average of the mean discharge rate increases for all subjects with the exception of subjects one and two between the baseline recording and both the post-ZeroG and

post-control conditions. Subjects three, four, and five show an increase in the distribution of the mean discharge rate between the baseline and post-ZeroG recordings. No significant differences were found between any of the three conditions for any of the four features.

Figure 5 provides the z-score normalized values of the pooled motor units for each of the four features. This figure shows the jittered value of the data, as well as the box and whisker plots with the mean denoted by a cross and the inter-quartile means
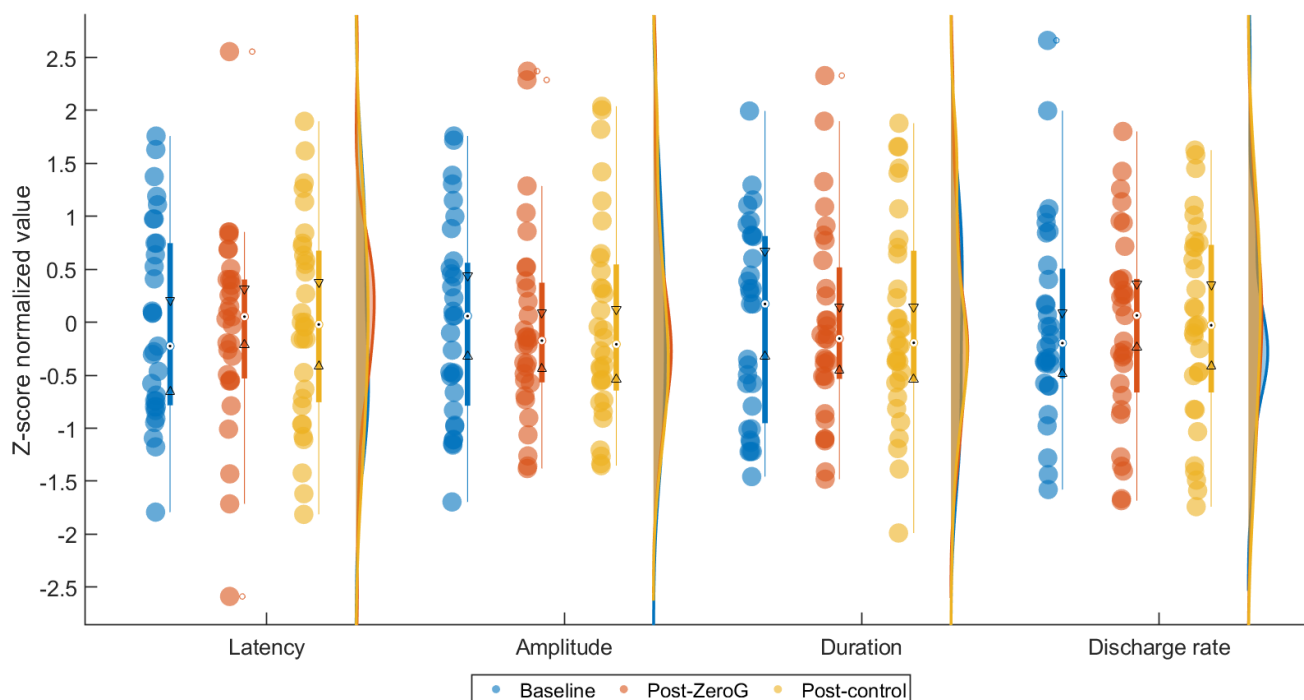

Fig. 5: Z-score normalized features of motor units pooled across subjects for all three conditions represented by jitter, box and whisker, and distribution plots per each condition and figure

denoted by triangles. The distribution is shown to the right of the respective jitter and box and whisker plots. When the normalized data is compared, the post-ZeroG values have less range than those of the baseline and post-control conditions for the latency and amplitude of the motor units. The mean increases for latency and discharge rate for both the post-control and post-ZeroG conditions, and decreases for both the amplitude and duration when compared with the mean baseline value. The latency, amplitude, and duration all show a more normal distribution for the post-ZeroG condition when compared with the other two conditions.

B. Tracked Motor units

One subject had motor units that could be tracked across all three conditions. Four other subjects had motor units that could be mapped across two conditions. No discernible trends were observed for any features other than latency. Looking into all twelve tracked motor units, it can be seen in Figure 6 that the greatest latency is observed in the post-ZeroG condition, while the lowest latency is observed in the baseline condition. The only exception is motor unit seven, which has a slightly larger latency in the post-control condition compared to the ZeroG condition. Similar figures for the amplitude, duration, and mean discharge rates of the tracked motor units may be examined in Appendix D.
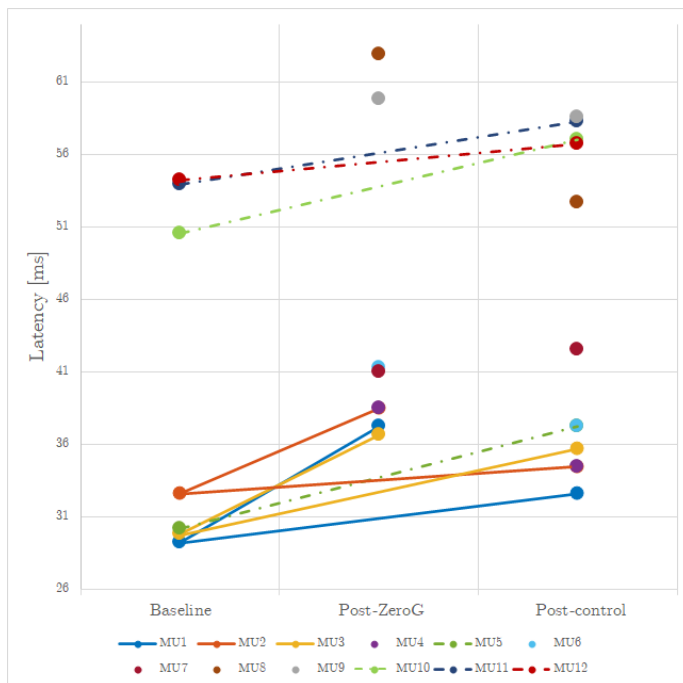

Fig. 6: Latency for all twelve MUs tracked across at least two conditions. MUs observed in only the baseline and control conditions are related with a dash-dot line. MUs observed in only the control and ZeroG conditions are not linked. MUs observed in all three conditions are related with a solid line

Figure 7 gives the values for all four features for the motor units tracked over all three conditions. It can be seen in Figure 7 that the latency of the stretch-reflex increases for both walking conditions, with the post-ZeroG latency being greater

than the post-control latency. The amplitude and duration both decrease for the two walking conditions for motor units one and two, however there is no notable difference between the post-ZeroG and post-control values. A slight decrease is seen in the mean discharge rate for motor units one and two the ZeroG condition, and a slight increase is seen in the same motor units for the post-control condition.
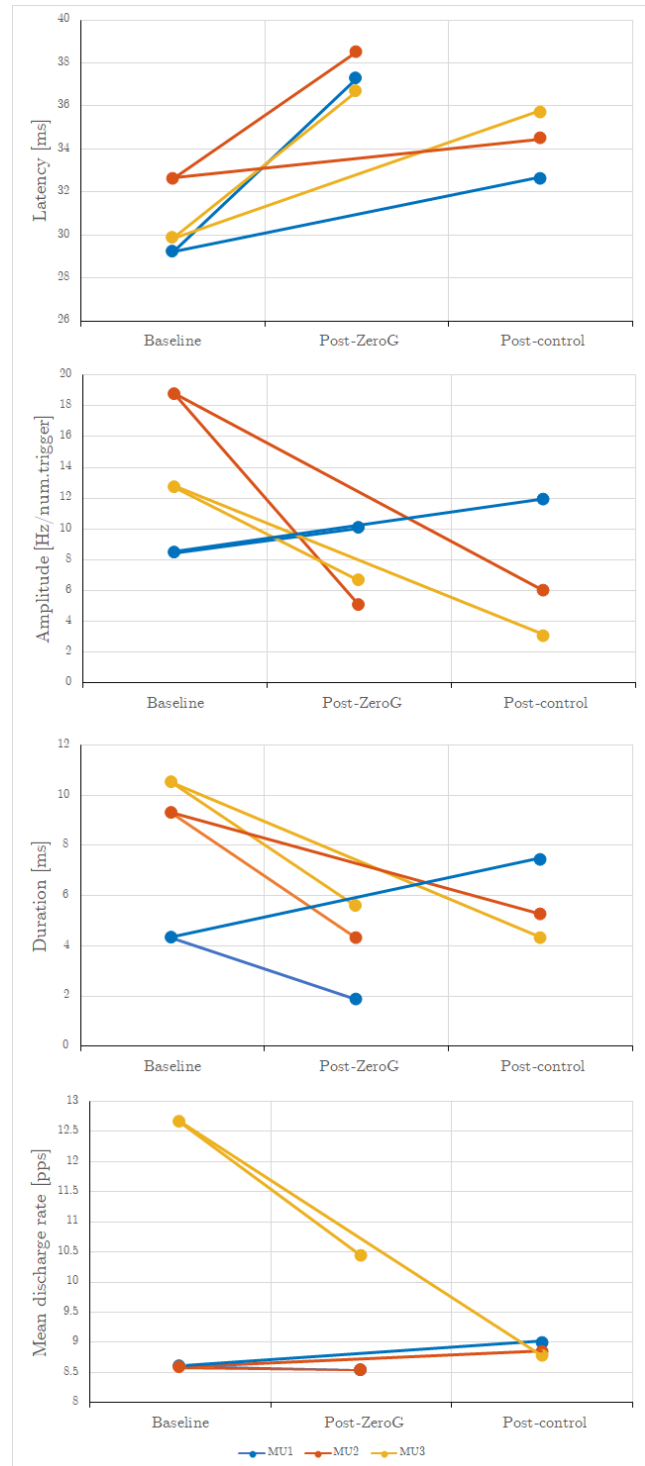

Fig. 7: From top to bottom: Latency, amplitude, duration, and mean discharge rate for the three tracked motor units for all three conditions

IV. DISCUSSION

The aim of this study was to develop a methodology that would be able to elicit and observe the underlying neurophysiological adaptations to short-term body-weight support training. The proposed methodology was comprised of three portions, the data recording phase, BWS walking using the ZeroG, and unassisted treadmill walking. During the data recordings, a perturbation protocol was administered, with the subject undergoing approximately 75 ankle dorsiflexion perturbations while the subject maintained an isometric contraction of 20% MVC. It was expected that the use of HD-EMG in conjunction with CKC decomposition methods would make it possible to observe adaptations to short-term body-weight support training in the soleus short-latency stretch reflex. While no significant results were found in the pooled motor unit analyses, changes could be found in the latency of individual motor units tracked across the three separate conditions.

In total, 31 motor units were pooled for the baseline condition and ZeroG conditions, and 32 motor units were pooled for the control condition. After Z-normalizing the data, three motor units (two from Subject 6 and one from Subject 3) were excluded from the post-control pool due to insufficient data points for the normalization. Two motor units from Subject 6 were excluded from the post-ZeroG pool for the same reason. For the Z-normalized data, the mean amplitude and duration decrease for both the post-ZeroG and control conditions when compared to the baseline recording. The average latency and mean discharge rate both increase for the post-ZeroG and control conditions when compared to the baseline. The increase was greater for the post-ZeroG than the post-control for all four features. It is also interesting to note that while no significant change in the value of the observed data was found between the different conditions, the Z-normalized data did assume a more normal distribution for all four features after the post-ZeroG and post-control conditions. The latency shows greater normality for the post-ZeroG condition than for the post-control condition. This indicates that variance in motor unit behaviour could be decreased through treadmill walking.

The analysis of motor units tracked across all three conditions showed limited but promising results. Three motor units for a single subject were tracked across all three conditions. These three motor units showed an increase in latency for both the ZeroG and control conditions when compared to the baseline. This increase in latency was slightly larger for the ZeroG condition, an average increase of 6.9ms $\pm$ 1.1ms, compared to the control which had an average increase of 3.7ms $\pm$ 2.0 ms. Nine further motor units, seven of which were obtained from three other subjects, were tracked across only two conditions. These motor units agree with the trend in latency seen in the first three motor units. The latency is greater for all but one motor unit after the baseline when compared to either the ZeroG or baseline condition. Ankle angle has been shown to affect the latency of motor units in

seated humans, with the latency increasing with the degree of plantar flexion [38]. However, as the ankle angle was held constant for all subjects across all recordings, the cause for this increase may be due to a decrease in the sensitivity of the muscle spindle. It has been suggested that changes in muscle spindle sensitivity may influence the latency of the soleus muscle [23]. An increase in latency such as that seen in the tracked motor units may be due to the introduction of slack in intrafusal fibres, as this slack must first be shortened before the muscle spindle could begin to respond [38][39]. Simulated microgravity has been shown to decrease tendon stiffness, and it may be that short-term gravity compensation already evokes slight tendon compliance [40]. The decrease in amplitude and duration after the walking taks observed in tracked motor units one and two suggests that fatigue may be another contributing factor to the concurrent increase in latency [41]. However, this decrease was only observed in three of the seven motor units that could be tracked between the baseline recording and at least one walking condition. An examination of the motor unit discharge rates over time found that fatigue likely was not a contributing factor, however an analysis of the EMG data for the possible influence of fatigue should be additionally performed to conclusively rule this out. This examination was not performed in this thesis due to time constraints. No discernible trends were observed for any of the three other features when examining all twelve tracked motor units. This could change with an increased pool of tracked motor units, which could be achieved by improving the methodology to decrease noise and improve motor unit decomposition. The presence of a trend in the latency of the tracked motor units suggests that investigating the modulation of individual motor units may provide insights otherwise obscured by the high variability of motor unit behaviour when pooled [42].

Based on previous studies that used HD-EMG for motor unit decomposition, it was expected that approximately five to fifteen motor units could be decomposed per subject per condition [24][25]. Due to the small surface area of the soleus muscle, this is of course fewer motor units than would be expected for larger muscles such as the tibialis anterior. While some subjects had more motor units found in this study, these were not included in the analysis due to noise obscuring the stretch reflex. The need to resample the data is assumed to be the cause for the fewer motor units successfully decomposed in this study. This assumption is corroborated by the results of Subject 5. The baseline recording for Subject 5 is the only data that did not require resampling, and 13 motor units were decomposed for this condition, compared to five and seven motor units being decomposed for the post-ZeroG and post-control conditions respectively. The greatest concern with the application of the resampling process was the introduction of uncertainty into the timing of the reflex. Subject 5 provides insight into this, with the resampled and original data both being within similar time ranges with the baseline ranging from 47-57ms, post-ZeroG from 48-53ms, and post-control from 55-58ms. The latency ranged between 31ms and 65ms across patients

and recordings, which is slightly outside the expected range of approximately 35-50ms [20][43].

It is worth noting that discharge rate, duration, and amplitude have all been shown to be modulated with contraction force, and as such it was unlikely to see changes in these features when the contraction force was held constant [24][25]. Changes in the soleus H-reflex before and after short-term body-weight or exoskeleton training have so far only been recorded in subjects with spinal cord injury, such as in a study from Phadke et. al, where the H-reflex was measured during swing-phase in both uninjured controls and subjects with SCI [26]. Previous studies have thoroughly examined the H-reflex with both exoskeleton and body-weight support for short-term training, and have found no statistically significant changes after training with either device [14][44]. It was expected that the use of high-density EMG would provide greater insight into the motor unit behaviour than would be possible using intramuscular EMG due to the potential for decomposing a greater number of motor units per subject. However, while statistically significant results were not found, several insights into improving the methodology in order to improve the results were developed.

This study could be refined through the reduction of uncertainties in the methodology. A separate study into the amount of time using the ZeroG at 40% weight compensation is required to reduce muscle activation could verify the assumption that body-weight support reduces muscle activation by approximately twenty percent in a similar time frame to a lower-limb exoskeleton. Previous literature evaluating the effect of body-weight support on muscle activation were able to observe a reduction in activation in a matter of minutes, with Kristiansen et al using only two minutes, and Maclean and Ferris using eight minutes [11][44]. This indicates that while there was likely a reduction in muscle activation during this study, it may not have been at the desired 20% threshold. The measurement of EMG during the walking sections could also be recorded in future studies. This could allow for greater control of the muscle activation level, as well as provide further insight into the motoneuron behaviour during walking. This methodology was considered for this thesis, however was ultimately rejected due to the potential for the EMG sensors to slip or come unstuck during walking due to the subject's sweat and movement. The use of wireless EMG sensors may allow for this adaptation to future studies, as removing the influence of the cables on the sensors' position could allow them to retain their position for the entirety of the walking task.

A further improvement to this study would be to simplify the tracking task. This would achieve two purposes, improving the efficiency of the underlying code, which would likely remove the delayed signal recording seen in this study. The second outcome would be to potentially improve the ability of the subject to more accurately follow the task, by providing a simpler goal such as increasing applying pressure to raise a bar until it reaches a certain point. Removing the need to resample the EMG data in post-processing would allow for more certainty regarding the timing of the reflex and increase confidence in the between-trial results per subject.

This study indicates that further investigation into the modulation of individual motor units may hold the key to understanding motor unit adaptations to rehabilitative gait training. An increased subject pool and refinements of the methodology to reduce noise could build on this thesis towards a greater understanding of the modulation of motor units to short-term body-weight support training.

REFERENCES

[1] V. L. Feigin, T. Vos, E. Nichols, M. O. Owolabi, W. M. Carroll, M. Dichgans, G. Deuschl, P. Parmar, M. Brainin, and C. Murray, "The global burden of neurological disorders: translating evidence into policy," *The Lancet Neurology*, vol. 19, pp. 255–265, 3 2020.

[2] T. Pringsheim, K. Fiest, and N. Jette, "The international incidence and prevalence of neurologic conditions: How common are they?," *Neurology*, vol. 83, pp. 1661–1664, 10 2014.

[3] J. M. Belda-Lois, S. Mena-Del Horno, I. Bermejo-Bosch, J. C. Moreno, J. L. Pons, D. Farina, M. Iosa, M. Molinari, F. Tamburella, A. Ramos, A. Caria, T. Solis-Escalante, C. Brunner, and M. Rea, "Rehabilitation of gait after stroke: A review towards a top-down approach," 2011.

[4] T. Mikolajczyk, I. Ciobanu, D. I. Badea, A. Iliescu, S. Pizzamiglio, T. Schauer, T. Seel, P. L. Seiciu, D. L. Turner, and M. Berteanu, "Advanced technology for gait rehabilitation: An overview," *Advances in Mechanical Engineering*, vol. 10, 7 2018.

[5] M. Gandolfi, N. Valè, F. Posteraro, G. Morone, A. Dell'orco, A. Botticelli, E. Dimitrova, E. Gervasoni, M. Goffredo, J. Zenzeri, A. Antonini, C. Daniele, P. Benanti, P. Boldrini, D. Bonaiuti, E. Castelli, F. Draicchio, V. Falabella, S. Galeri, F. Gimigliano, M. Grigioni, S. Mazzon, F. Molteni, M. Petrarca, A. Picelli, M. Senatore, G. Turchetti, D. Giansanti, and S. Mazzoleni, "State of the art and challenges for the classification of studies on electromechanical and robotic devices in neurorehabilitation: A scoping review," 10 2021.

[6] A. Loro, M. B. Borg, M. Battaglia, A. P. Amico, R. Antenucci, P. Benanti, M. Bertoni, L. Bissolotti, P. Boldrini, D. Bonaiuti, T. Bowman, M. Capecci, E. Castelli, L. Cavalli, N. Cinone, L. Cosenza, R. Di Censo, G. Di Stefano, F. Draicchio, V. Falabella, M. Filippetti, S. Galeri, F. Gimigliano, M. Grigioni, M. Invernizzi, J. Jonsdottir, C. Lentino, P. Massai, S. Mazzoleni, S. Mazzon, F. Molteni, S. Morelli, G. Morone, A. Nardone, D. Panzeri, M. Petrarca, F. Posteraro, A. Santamato, L. Scotti, M. Senatore, S. Spina, E. Taglione, G. Turchetti, V. Varalta, A. Picelli, and A. Baricich, "Balance Rehabilitation through Robot-Assisted Gait Training in Post-Stroke Patients: A Systematic Review and Meta-Analysis," *Brain Sciences*, vol. 13, p. 92, 1 2023.

[7] T. Lam, J. Eng, D. Wolfe, J. Hsieh, and M. Whittaker, "A Systematic Review of the Efficacy of Gait Rehabilitation

Strategies for Spinal Cord Injury," *Topics in Spinal Cord Injury Rehabilitation*, vol. 13, pp. 32–57, 7 2007.

[8] A. K. Bonkhoff and C. Grefkes, "Precision medicine in stroke: towards personalized outcome predictions using artificial intelligence," *Brain*, vol. 145, pp. 457–475, 4 2022.

[9] D. Rotstein and X. Montalban, "Reaching an evidence-based prognosis for personalized treatment of multiple sclerosis," *Nature Reviews Neurology*, vol. 15, pp. 287–300, 5 2019.

[10] J. Hidler, D. Brennan, i. Black, D. Nichols, K. Brady, and T. Nef, "ZeroG: Overground gait and balance training system," *The Journal of Rehabilitation Research and Development*, vol. 48, no. 4, p. 287, 2011.

[11] M. Kristiansen, N. Odderskær, and D. H. Kristensen, "Effect of body weight support on muscle activation during walking on a lower body positive pressure treadmill," *Journal of Electromyography and Kinesiology*, vol. 48, pp. 9–16, 10 2019.

[12] A. C. Smith, W. Z. Rymer, and M. Knikou, "Locomotor training modifies soleus monosynaptic motoneuron responses in human spinal cord injury," *Experimental Brain Research*, vol. 233, pp. 89–103, 1 2015.

[13] M. Knikou, A. C. Smith, and C. K. Mummidisetty, "Locomotor training improves reciprocal and nonreciprocal inhibitory control of soleus motoneurons in human spinal cord injury," *Journal of Neurophysiology*, vol. 113, pp. 2447–2460, 4 2015.

[14] P.-C. Kao, C. L. Lewis, and D. P. Ferris, "Short-term locomotor adaptation to a robotic ankle exoskeleton does not alter soleus Hoffmann reflex amplitude," tech. rep., 2010.

[15] K. E. Gordon and D. P. Ferris, "Learning to walk with a robotic ankle exoskeleton," *Journal of Biomechanics*, vol. 40, no. 12, pp. 2636–2644, 2007.

[16] L. Zhou, W. Chen, W. Chen, S. Bai, J. Zhang, and J. Wang, "Design of a passive lower limb exoskeleton for walking assistance with gravity compensation," *Mechanism and Machine Theory*, vol. 150, p. 103840, 8 2020.

[17] A. L. Hicks, M. M. Adams, K. Martin Ginis, L. Giangregorio, A. Latimer, S. M. Phillips, and N. McCartney, "Long-term body-weight-supported treadmill training and subsequent follow-up in persons with chronic SCI: effects on functional walking ability and measures of subjective well-being," *Spinal Cord*, vol. 43, pp. 291–298, 5 2005.

[18] N. Mrachacz-Kersting, M. J. Grey, and T. Sinkjær, "Evidence for a supraspinal contribution to the human quadriceps long-latency stretch reflex," *Experimental Brain Research*, vol. 168, pp. 529–540, 1 2006.

[19] X. N. Mrachacz-Kersting, U. G. Kersting, X. P. De Brito Silva, Y. Makihara, L. Arendt-Nielsen, T. Sinkjaer, and X. A. K. Thompson, "Acquisition of a simple motor skill: task-dependent adaptation and long-term changes in the human soleus stretch reflex," *J Neurophysiol*, vol. 122, pp. 435–446, 2019.

[20] M. J. Grey, M. Ladouceur, J. B. Andersen, J. B. Nielsen, and T. Sinkjær, "Group II muscle afferents probably contribute to the medium latency soleus stretch reflex during walking in humans," *The Journal of Physiology*, vol. 534, pp. 925–933, 8 2001.

[21] A. K. Thompson, Y. C. Xiang, and J. R. Wolpaw, "Acquisition of a simple motor skill: Task-dependent adaptation plus long-term change in the human soleus H-reflex," *Journal of Neuroscience*, vol. 29, pp. 5784–5792, 5 2009.

[22] R. M. Palmieri, . Christopher, D. Ingersoll, and M. A. Hoffman, "by the National Athletic Trainers," Tech. Rep. 3, 2004.

[23] T. Sinkjaer, J. B. Andersen, and B. Larsen, "Soleus stretch reflex modulation during gait in humans," *Journal of Neurophysiology*, vol. 76, pp. 1112–1120, 8 1996.

[24] U. S. Yavuz, F. Negro, O. Sebik, A. Holobar, C. Frömmel, K. S. Türker, and D. Farina, "Estimating reflex responses in large populations of motor units by decomposition of the high-density surface electromyogram," *Journal of Physiology*, vol. 593, pp. 4305–4318, 10 2015.

[25] J. Kallio, K. Søgaard, J. Avela, P. V. Komi, H. Selänne, and V. Linnamo, "Motor Unit Firing Behaviour of Soleus Muscle in Isometric and Dynamic Contractions," *PLoS ONE*, vol. 8, 2 2013.

[26] C. P. Phadke, S. S. Wu, F. J. Thompson, and A. L. Behrman, "Comparison of Soleus H-Reflex Modulation After Incomplete Spinal Cord Injury in 2 Walking Environments: Treadmill With Body Weight Support and Overground," *Archives of Physical Medicine and Rehabilitation*, vol. 88, pp. 1606–1613, 12 2007.

[27] C. K. Thompson, F. Negro, M. D. Johnson, M. R. Holmes, L. M. McPherson, R. K. Powers, D. Farina, and C. J. Heckman, "Robust and accurate decoding of motoneuron behaviour and prediction of the resulting force output," *The Journal of Physiology*, vol. 596, pp. 2643–2659, 7 2018.

[28] "Analysis of motor unit spike trains estimated from high-density surface electromyography is highly reliable across operators," 2021.

[29] Y. Peng, J. He, B. Yao, S. Li, P. Zhou, and Y. Zhang, "Motor unit number estimation based on high-density surface electromyography decomposition," *Clinical Neurophysiology*, vol. 127, pp. 3059–3065, 9 2016.

[30] J. M. Shefner, "Motor unit number estimation in human neurological diseases and animal models," *Clinical Neurophysiology*, vol. 112, pp. 955–964, 6 2001.

[31] K. G. Keenan, D. Farina, R. Merletti, and R. M. Enoka, "Amplitude cancellation reduces the size of motor unit potentials averaged from the surface EMG," *Journal of Applied Physiology*, vol. 100, pp. 1928–1937, 6 2006.

[32] A. Holobar and D. Zazula, "LNCS 4666 - Gradient Convolution Kernel Compensation Applied to Surface Electromyograms," tech. rep.

[33] I. Karacan, H. I. Cakar, O. Sebik, G. Yilmaz, M. Cidem, S. Kara, and K. S. TÃ¼rker, "A new method to determine reflex latency induced by high rate stimulation of the nervous system," *Frontiers in Human Neuroscience*, vol. 8, 7 2014.

[34] A. Del Vecchio, A. Holobar, D. Falla, F. Felici, R. Enoka, and D. Farina, "Tutorial: Analysis of motor unit discharge characteristics from high-density surface EMG signals," *Journal of Electromyography and Kinesiology*, vol. 53, p. 102426, 8 2020.

[35] N. Davey, P. Ellaway, and R. Stein, "Statistical limits for detecting change in the cumulative sum derivative of the peristimulus time histogram," *Journal of Neuroscience Methods*, vol. 17, pp. 153–166, 8 1986.

[36] E. Martinez-Valdes, F. Negro, C. M. Laine, D. Falla, F. Mayer, and D. Farina, "Tracking motor units longitudinally across experimental sessions with high-density surface electromyography," *The Journal of Physiology*, vol. 595, pp. 1479–1496, 3 2017.

[37] P. Contessa, C. J. De Luca, and J. C. Kline, "The compensatory interaction between motor unit firing behavior and muscle force during fatigue," *Journal of Neurophysiology*, vol. 116, pp. 1579–1585, 10 2016.

[38] S. J. Fellows and A. F. Thilmann, "Experimental Brain Research The role of joint biomechanics in determining stretch reflex latency at the normal human ankle," tech. rep., 1989.

[39] G. L. Gottlieb, G. C. Agarwal, and R. J. Jaeger, "Response to sudden torques about ankle in man. IV. A functional role of alpha-gamma linkage.," *Journal of Neurophysiology*, vol. 46, pp. 179–190, 7 1981.

[40] Y. A. Koryak, "Influence of simulated microgravity on mechanical properties in the human triceps surae muscle in vivo. I: Effect of 120 days of bed-rest without physical training on human muscle musculo-tendinous stiffness and contractile properties in young women," *European Journal of Applied Physiology*, vol. 114, pp. 1025–1036, 5 2014.

[41] R. Kuchinad, T. Ivanova, and S. Garland, "Modulation of motor unit discharge rate and H-reflex amplitude during submaximal fatigue of the human soleus muscle," *Experimental Brain Research*, vol. 158, 10 2004.

[42] C. T. Moritz, B. K. Barry, M. A. Pascoe, and R. M. Enoka, "Discharge Rate Variability Influences the Variation in Force Fluctuations Across the Working Range of a Hand Muscle," *Journal of Neurophysiology*, vol. 93, pp. 2449–2459, 5 2005.

[43] T. Sinkjær, J. B. Andersen, J. F. Nielsen, and H. J. Hansen, "Soleus long-latency stretch reflexes during walking in healthy and spastic humans," *Clinical Neurophysiology*, vol. 110, pp. 951–959, 5 1999.

[44] M. K. MacLean and D. P. Ferris, "Human muscle activity and lower limb biomechanics of overground walking at varying levels of simulated reduced gravity and gait speeds," *PLoS ONE*, vol. 16, 7 2021.

A. *Resampling methodology*

During the post-processing synchronization of the Achilles and EMG signals, a lag was observed in the EMG data. It can be seen in Figure 8 that the EMG signal records a perturbation prior to the Achilles signal at the beginning of the recording, however the EMG signal lags increasingly until the EMG signal shows the perturbation after the Achilles signal.
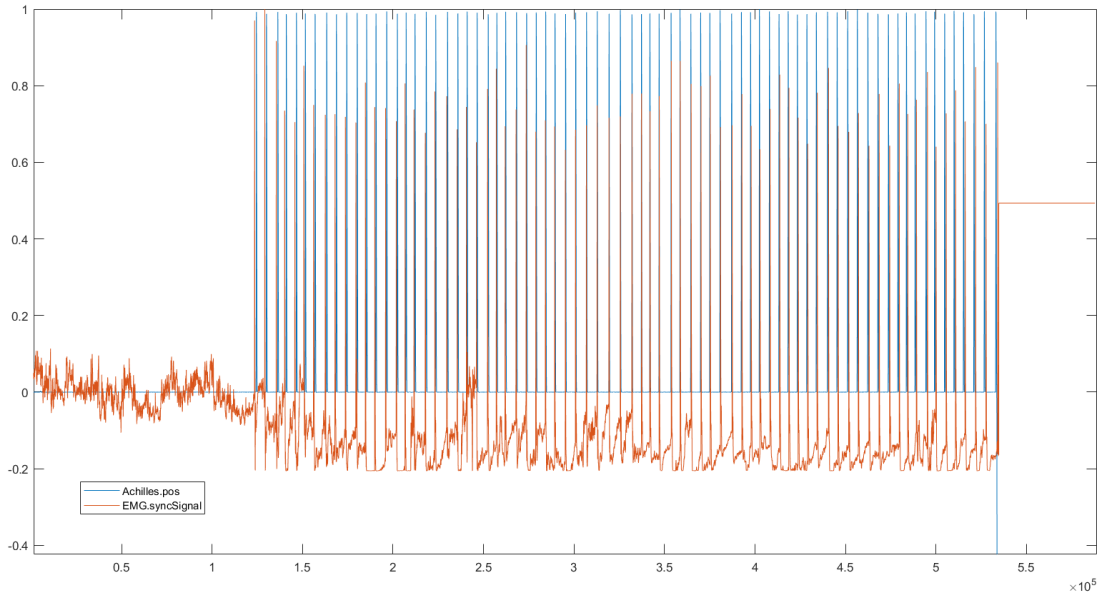

Fig. 8: Comparison of Achilles sync signal and the EMG synchronization signal

Files with a lag in the synchronization signal were resampled by segments. The two synchronization signals were used to determine the size of the lag between the REFA and the Achilles. The REFA data was then segmented into sections between the peaks in the synchronization signal, and resampled using the MATLAB "resample" function. This function uses an FIR anti-aliasing lowpass filter on the input signal, in this case, the respective EMG signals. Each segment of the EMG data is resampled by multiplying the relevant signal by the ratio of the number of data points in the Achilles synchronization signal segment, divided by the number of data points in the REFA synchronization signal segment. The relevant mathematics as written in MATLAB are as follows:

```
function resamped = resampleData(data,AchSync,EMGSync,fs)
a=detrend(EMGSync,0);
b = detrend(AchSync,0);
% Locate perturbations
[pk,EMG_ind]=findpeaks(a,'MINPEAKHEIGHT',max(a)*40/100,'MINPEAKDISTANCE',0.5*fs);
[pk,Ach_ind]=findpeaks(b,'MINPEAKHEIGHT',max(b)*40/100,'MINPEAKDISTANCE',0.5*fs);

% Initialize arrays for resampled data and include data prior to first perturbation
resamped.delayTrend = delay;
resamped.EMGSync = EMGSync(1:EMG_ind(1));
resamped.EMG     = data(1:EMG_ind(1),:);

% Resample data
for j = 1:length(delay)-1
    if delay(j) < 0
        resamped.EMGSync = [resamped.EMGSync; resample(EMGSync(EMG_ind(j):EMG_ind(j+1))...
                          ,(Ach_ind(j+1)-Ach_ind(j)),(EMG_ind(j+1)-EMG_ind(j))+1)];
        resamped.EMG = [resamped.EMG; resample(data(EMG_ind(j):EMG_ind(j+1),:)...
                      ,(Ach_ind(j+1)-Ach_ind(j)),(EMG_ind(j+1)-EMG_ind(j))+1)];
    else
        resamped.EMGSync = [resamped.EMGSync;resample(EMGSync(EMG_ind(j):EMG_ind(j+1))...
                          ,(Ach_ind(j+1)-Ach_ind(j))+1,(EMG_ind(j+1)-EMG_ind(j))+1)];
```

```
        resamped.EMG = [resamped.EMG; resample(data(EMG_ind(j):EMG_ind(j+1),:)...
                    ,(Ach_ind(j+1)-Ach_ind(j))+1,(EMG_ind(j+1)-EMG_ind(j))+1)];
    end
end

[~,new_ind] = findpeaks(resamped.EMGSync,'MINPEAKHEIGHT',max(resamped.EMGSync)*40/100,...
            'MINPEAKDISTANCE',0.5*fs);
resamped.delay = Ach_ind(1)-new_ind(1);

end
```

B. Peri-stimulus analysis

The four figures used for analyzing the averaged motor unit reflex are shown in Figure 9. The M1 and M2 reflexes are indicated, with the onset and plateau of the M1 reflex shown in the PSF cumulative sum graph being used to calculate the latency, amplitude, duration, and mean discharge rate for each decomposed motor unit.
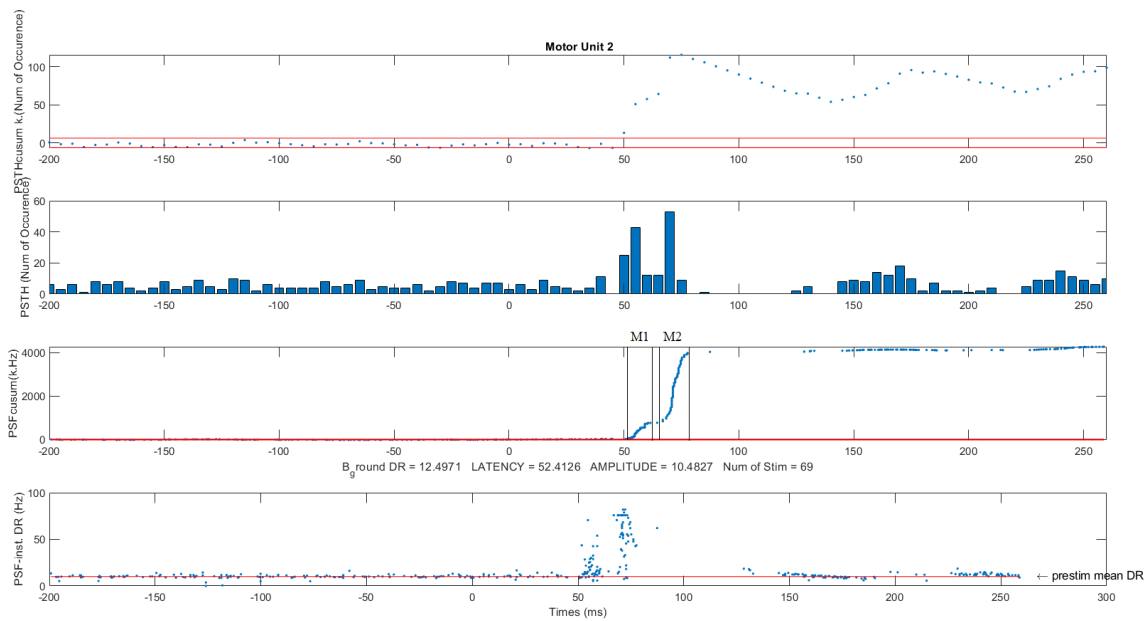

Fig. 9: Peri-stimulus analysis for a single motor unit. The sub-figures show from top to bottom: peri-stimulus cumulative sum time histogram (PSTHC), peri-stimulus time histogram (PSTH), peri-stimulus cumulative sum frequency-gram (PSFC), and peri-stimulus frequency-gram (PSF). The M1 and M2 reflexes are indicated on the PSFC

C. Tracked Motor Units: Analysis

Figure 10 shows the comparison of action potentials for two motor units from separate conditions (baseline and post-ZeroG) with a cross-correlation of 94%. Dead channels have been removed, resulting in only 61 channels being displayed.
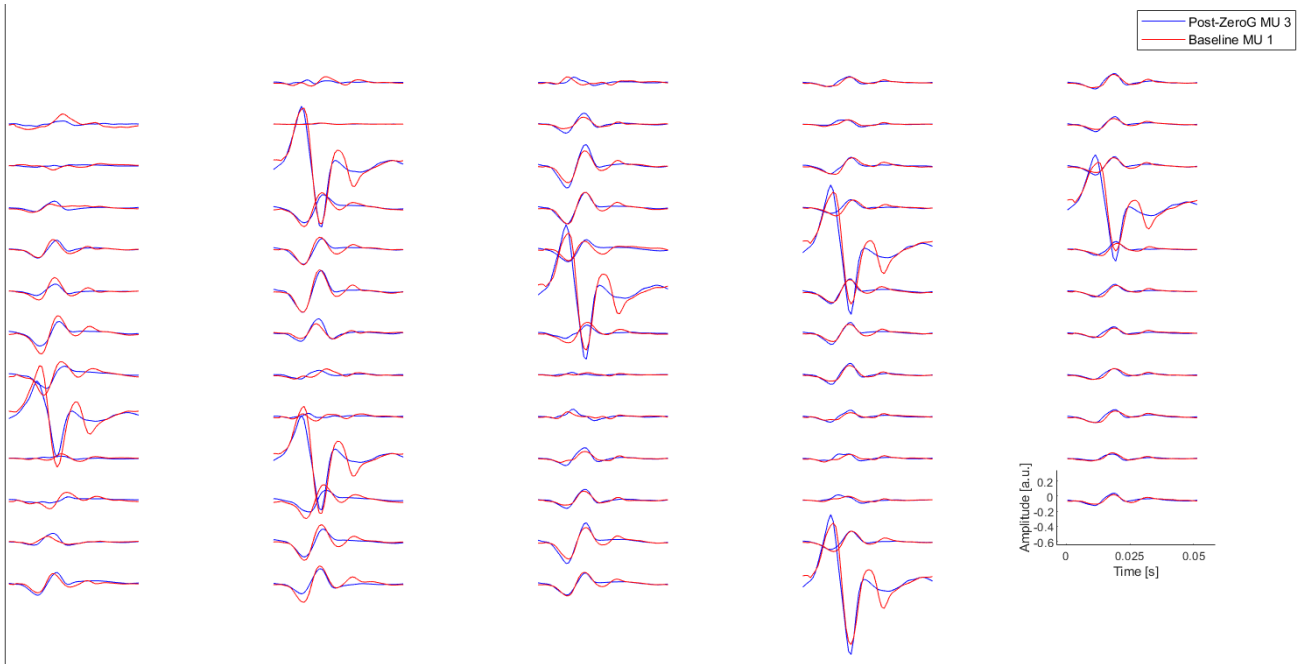

Fig. 10: Comparison of averaged action potentials between motor units from the post-ZeroG and baseline conditions for subject 1 for each active HD-EMG channel. The last channel shows the axes for each of the generated waveforms

The outcome of a comparison between two conditions for a subject is exemplified in Table I. In this table, it can be seen that there are multiple matches above the 85% threshold for the same motor unit. In this instance, the motor unit with the highest cross-correlation value will be selected. In this example, the bold-ed motor units are considered to be matches.

TABLE I: Example of output from motor unit matching analysis showing the results from the post-ZeroG and baseline conditions for subject 1

Post-ZeroG MU no.	Baseline MU no.	Cross-correlation
1	**4**	**0.986498**
2	2	0.670222
3	**1**	**0.940327**
4	4	0.940897
5	**3**	**0.893971**
6	1	0.731418
7	1	0.879175
8	4	0.672965
9	1	0.603152
10	4	0.920998

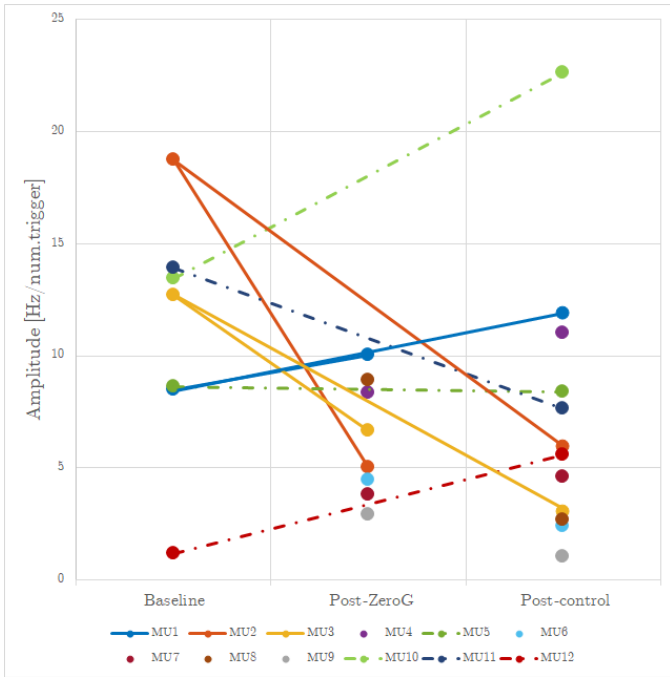## D. Tracked Motor Units: Results

Fig. 11: Amplitude for all twelve MUs tracked across at least two conditions. MUs observed in only the baseline and control conditions are related with a dash-dot line.MUs observed in only the control and ZeroG conditions are not linked. MUs observed in all three conditions are related with a solid line
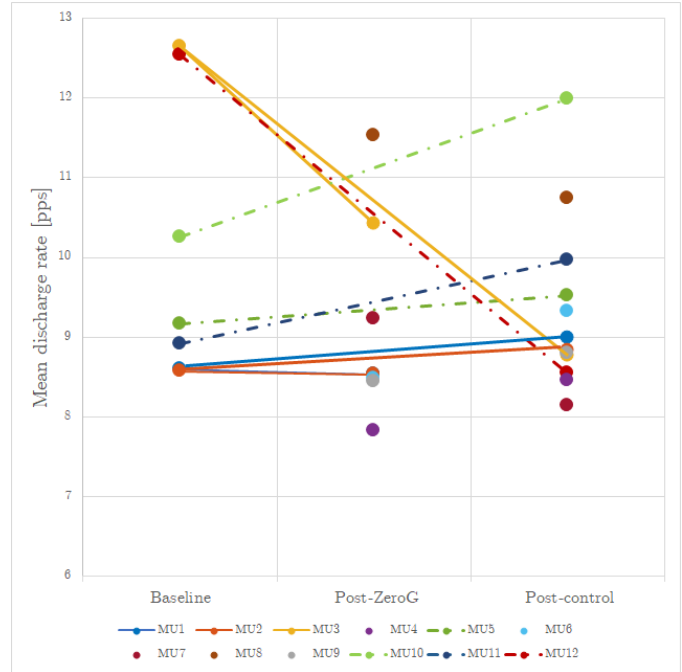

Fig. 13: Mean discharge rate for all twelve MUs tracked across at least two conditions. MUs observed in only the baseline and control conditions are related with a dash-dot line.MUs observed in only the control and ZeroG conditions are not linked. MUs observed in all three conditions are related with a solid line
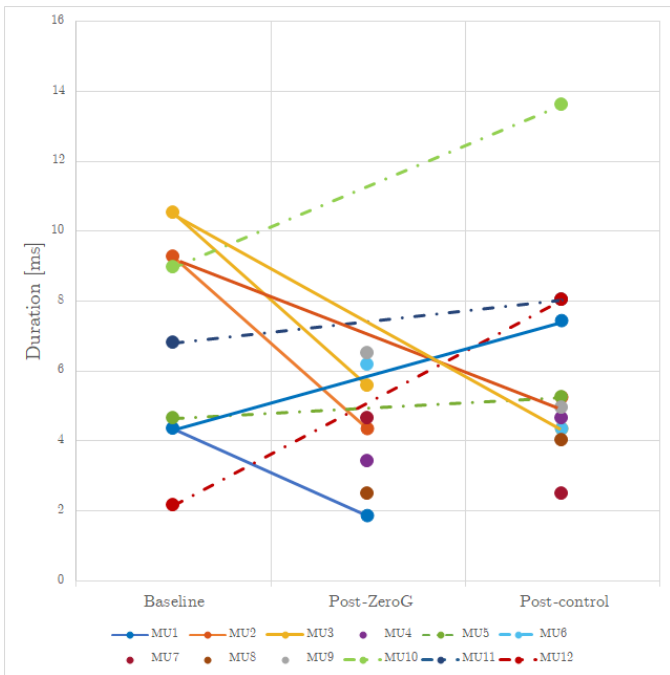

Fig. 12: Duration for all twelve MUs tracked across at least two conditions. MUs observed in only the baseline and control conditions are related with a dash-dot line.MUs observed in only the control and ZeroG conditions are not linked. MUs observed in all three conditions are related with a solid line